05

Spectrum of oscillation of the array of Josephson junctions in the coplanar line

© F.V. Khan,[1,2] L.V. Filippenko,[1] M.Yu. Fominsky,[1] A.B. Ermakov,[1] A.P. Orlov,[1] V.P. Koshelets[1]

[1] Kotelnikov Institute of Radio Engineering and Electronics, Russian Academy of Sciences,
125009 Moscow, Russia
[2] Moscow Institute of Physics and Technology (National Research University),
141701 Dolgoprudny, Moscow Region, Russia
e-mail: khanfv@hitech.cplire.ru

Received April 30, 2025
Revised April 30, 2025
Accepted April 30, 2025

We have studied spectral characteristics of radiation of an oscillator based on the array of Josephson junctions and evaluated its applicability as a heterodyne included in the superconducting integrated receiver. The array is 350 serial junctions that are embedded into a central electrode of the coplanar line. Radiation from the array is mixed with higher synthesizer harmonics (the frequency is 16−19 GHz) that originate in a single tunnel Josephson junction (a harmonic mixer). A signal at the difference frequency (up to 800 MHz) is output to a commercial spectrum analyzer. A natural width of the oscillation line in the best point was below 1 MHz with the signal-to-noise ration of 26.3 dB. The estimates of the line width within the model that takes into account noises of Josephson junctions as well as thermal and low-frequency noises are in qualitative agreement with experimental results. Besides, we were the first to implement a phase-locked loop mode to the stable external synthesizer in all the points, where the line width does not exceed 15 MHz.

Keywords: superconducting integrated receiver, heterodyne, Josephson junction, coplanar line, noises, phase-locked loop.

DOI: 10.61011/TP.2025.09.61925.87-25

Introduction

Superconductor electronics devices based on superconductor-insulator-superconductor (SIS) tunnel junctions are widely applied in various field of science and engineering. Thus, the main element of terahertz and subterahertz heterodyne receiver systems that are based on ground [1,2] and in space [3,4] at the frequencies of up to 1.2 THz is a signal mixer based on the tunnel SIS junction. The noise temperature of these devices approaches a value of the quantum limit: $T_n = hf/2k_B$, while the initial signal is transformed into the intermediate frequency with enhancement [5,6]. Here, f is a frequency of an arriving signal, while h and k_B are the Planck constant and the Boltzmann constant, respectively. These effects are possible due to operation of the devices at cryogenic temperatures and unique nonlinearity of the SIS junction near the gap voltage V_g [7].

In addition to the mixing element, operation of the heterodyne receivers also requires a heterodyne oscillator. For this purpose, high harmonics of synthesizer radiation, which are obtained in a multiplier cascade [8], are used, but it is more preferable to use the heterodyne oscillator that is arranged in the same chip together with the mixer and a receiving antenna. This approach was implemented in the superconducting integrated receiver (SIR) [9]. A superconducting oscillator based on a distributed Josephson junction (DJJ) was used as the heterodyne. The SIR was tested in studies for investigation of the atmosphere in the TELIS device [9], in the gas spectroscopy [10] and for investigation of a human body in the terahertz range [11].

The DJJ is a tunnel SIS contact that is manufactured in one cycle with the SIS mixer. The DJJ size along one of the directions multiply exceeds the Josephson depth $\lambda_J = \sqrt{\Phi_0/2\pi\mu_0 j_c d}$, where Φ_0 — the quantum of the magnetic flux, μ_0 — magnetic susceptibility of vacuum, j_c — the density of the critical current, $d = d_0 + \lambda_1 \coth(d_1/\lambda_1) + \lambda_2 \coth(d_2/\lambda_2)$ — the effective thickness of the transmission Josephson line, d_0 — the tunnel barrier thickness, while λ_1 and λ_2 — the London depth of penetration of the magnetic field into the upper and lower electrodes, respectively, while d_1 and d_2 are their thicknesses. When applying the magnetic field in the plane of the DJJ tunnel barrier, the field starts penetrating the junction in the form of vortices. When transmitting the current through the junction, the vortices are moved. When the vortex reaches a DJJ edge, an energy quantum is emitted.

The operating frequency of the DJJ-based superconducting oscillator is retuned within a wide range up to 700 GHz (the niobium gap frequency). At the higher frequencies, oscillation is almost impossible in the DJJ due to strong absorption in the niobium electrode.

At the voltages below $V_g/3$, the DJJ operates in a resonance mode[12]. Due to formation of standing waves inside the DJJ, its current-voltage curve (CVC) exhibits current

steps that are called Fiske steps[13]. The autonomous width of the oscillation line in operating points on the steps is of a value of about 1 MHz, while between the steps it exceeds 10 MHz. Operation of the phase-locked loop system (PLL) requires that the oscillation line width shall be below 15 MHz, therefore, it is difficult to select the operating points when the voltages are between the steps. The step position can be controlled by means of the external magnetic field, therefore, in order to ensure a mode of continuous retuning of the DJJ oscillation frequency, the measurements are preceded by a procedure of searching the operating points with various values of the magnetic field and the current through the DJJ. Besides, the position of the operating points is changed during sample thermal cycling, therefore, after thermal cycling the procedure of searching the operating points shall be performed again.

At the voltages above $V_g/3$, the DJJ operates in a mode of viscous vortex flow („flux-flow“). In this mode, due to a self-pumping effect, absorption of waves that propagate through the DJJ greatly increases and there are no Friske steps. At the same time, the oscillation line width is enough for implementing the PLL [9].

Arrays of the tunnel Josephson junctions can be used as alternative heterodyne signal sources for the superconducting integrated receiver. The arrays can be also manufactured in one technological process together with the mixer and the receiving antenna and the arrays oscillation frequencies are also in the terahertz and subterahertz ranges. When a concerted load is connected to the array, the power of the output signal increases with the number of junctions N and can be up to tens of microwatts [14–16]. At the same time, the oscillation line width is reduced in inverse proportion to N and with autonomous oscillation it has a typical value of hundreds of kilohertz. Additionally, the arrays of the Josephson junctions that are manufactured as per well proved technologies Nb-Al/AlN-NbN and Nb-Al/AlO_x-Nb can operate at the frequencies of up to 900 GHz, which was demonstrated in the study [17].

In the recent article [18], the authors of the present study have proposed a topology of the arrays of the Josephson junctions and preliminarily studied characteristics of the samples at direct current. The present study investigates the spectral characteristics of the experimental samples and specific features that originate during oscillation. Section 1 describes the experimental samples. Section 2 tells us about a procedure of the measurements. The obtained results are discussed in Section 3.

1. Experimental samples

The studied structures have been manufactured as per a technological process that includes several stages of magnetron sputtering, mask electron-beam lithography and ion-plasma etching. The Nb-Al/AlN-NbN junctions with the tunnel current's density of 13 kA/cm^2 are formed by means of magnetron sputtering of niobium with subsequent aluminum sputtering and nitridation. The electrodes are formed by „for-explosion“ (lift-off) lithography that is used to remove sizes below 0.5 μm. Details of the technological process can be found, for example, in the study [19].

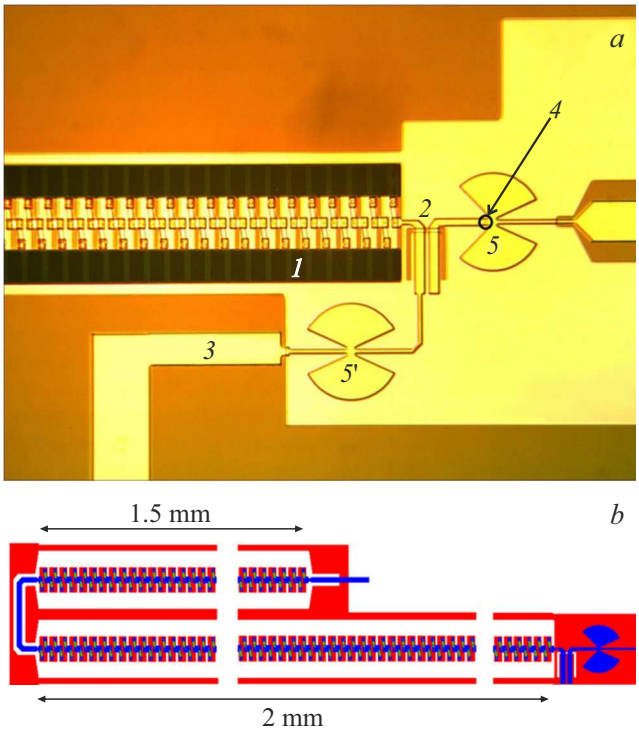

Figure 1. *a* — the image of the array and the SIS detector with an impedance transformer: *1* — the array of the Josephson junctions; *2* — the direct current gap between the array and the mixer on the SIS junction; *3* — the direct current line for array power supply; *4* — the harmonic SIS mixer; *5* — the radial contactor for detuning of capacitance of the SIS junction; *5′* — to prevent loss of the array power into its direct-current connect line (3); *b* — the drawing of the array that consists of 350 junctions.

An image of one of the studied samples is shown in Fig. 1, *a*. The array is N serial tunnel SIS junctions that are embedded into the central electrode of the coplanar line. In order to provide an unhysteretic progress of the array current-voltage curve, the junction is shunted by a thin-film resistor made of molybdenum which is in the normal condition at the liquid helium boiling temperature of 4.2 K. Synchronization between the junctions in the array is provided due to waves that propagate through the coplanar line. Fig. 1, *b* shows a drawing of the entire array with typical sizes.

In order to decrease outflow of power generated by the array, the direct-current power supply line *3* includes the radial contactor *5′* at the distance of $3\lambda/4$ from the direct-current gap *2*. Another radial contactor *5* is required to detune capacitance of the tunnel SIS junction *4*, that is used in a signal mixing circuit, from the array with the synthesizer harmonics at the high frequency. A fundamental frequency of the synthesizer f_{synth} is within the range from

16 to 19 GHz. A gap in the form of a slot antenna is required for independent direct-current connection of the array and a single SIS junction.

2. Procedure of the measurements

The studied sample is fixed to a holder of a measurement head and placed into a helium filled cryostat. An electrical contact of sample spots with power supply legs in the holder is implemented by means of a silver paste. In order to ensure a good thermal contact between a silicon substrate of the sample and a surface of the copper holder, a wax interlayer is done between them. For uniform contact on the entire contact area and for activation of the silver paste, the sample is placed in a furnace at the temperature of 50 °C.

The signal that obtained when mixing radiation of the array with the high harmonics of the synthesizer has a frequency from 0 to 800 MHz. It is supplied to amplifiers and after that one part of the signal is output to a spectrum analyzer's display and the other is supplied to a phase detector that controls the array voltage. The error signal from the phase detector is supplied to the array through a resistor of resistance of 50 Ω, which is near the chip in the cryostat. The phase detector shifts the operating point of the array in such a way as to eliminate a difference in the frequency and the phase between the difference frequency signal and the reference signal of the frequency of 400 MHz. Due to this, external phase synchronization occurs provided that the oscillation line width is below 15 MHz. This frequency is determined by a delay time in the phase synchronization loop.

All the components of a measurement bench are schematically shown in Fig. 2.

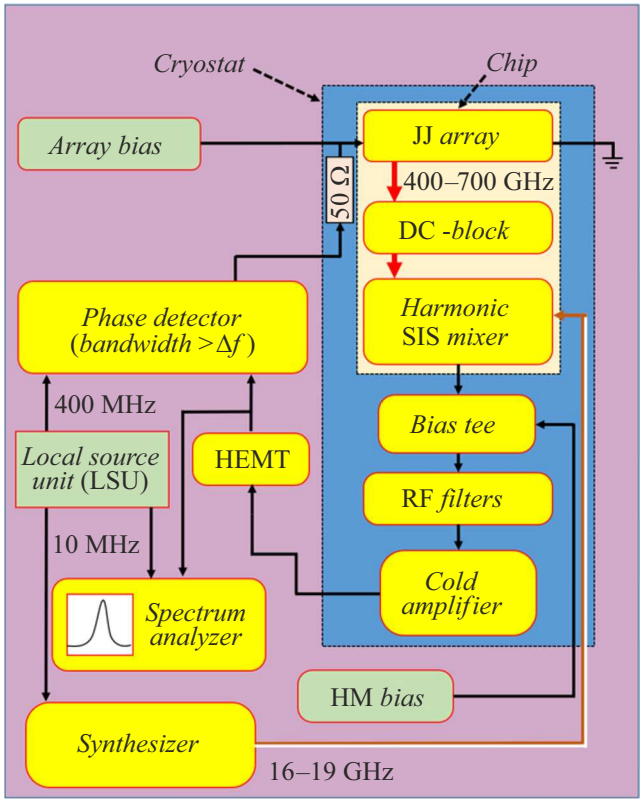

Figure 2. Experimental setup for investigating the oscillation line of the array of the Josephson junctions.

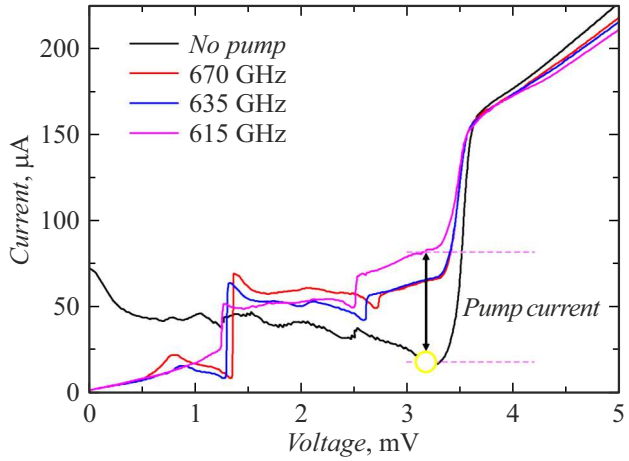

Figure 3. Current-voltage curve of the SIS mixer with oscillator pumping. The operating point around 3.1 mV is shown by a circle.

3. Results and discussion

3.1. Preliminary direct-current measurements

Under effect of the variable electromagnetic field that affects the SIS, there is an increase of probability of tunneling of quasi-particles at the voltages below V_g. This effect is called photon-assisted tunneling. At the same time, the current-voltage curve exhibits a series of the so-called quasi-particle current steps at the voltages $V = V_g - nhf/e$, where n is a number of photons of the frequency of f absorbed by the single photon and e is the charge of the electron. Due to unsuppressed critical current, at the voltages $V = phf/2e$ the current-voltage curve also exhibits the Shapiro steps, where p is an integer number. The current-voltage curve of the SIS junction when affected by the array signal is shown in Fig. 3.

The dependence of the pump current of the SIS junction on the frequency is shown in Fig. 4. As will be shown below, irregularity of the curve is most likely caused by capturing the array oscillation frequency when synchronizing the junctions near resonance mode of the coplanar line, in which the array is embedded. In practice, in order to effectively transform the oscillator signal to the difference frequency with subsequent capability of frequency and phase stabilization of the oscillation line, it is enough to have an output signal power that induces at the current-voltage curve of the SIS mixer a pump current that is equal to at least one tenth of the gap

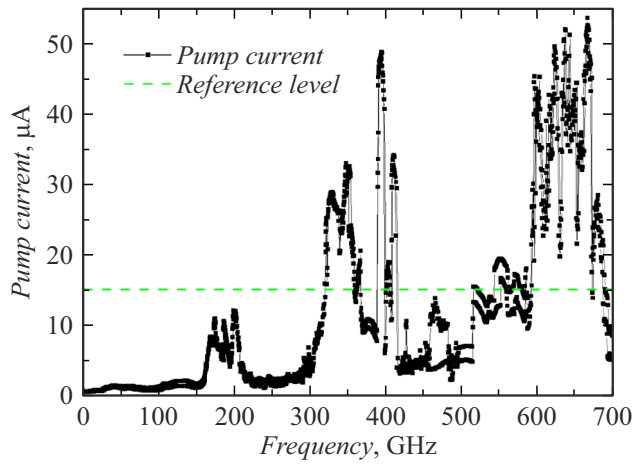

Figure 4. Dependence of the pump current on the frequency for the studied sample made up of 350 junctions. The maximum power that is determined from approximation of the current-voltage curve by expressions from the Tucker-Feldman model was about 0.12 μW. The points were taken when passing the current-voltage curve in forward and reverse directions. The green dashed line marks a pump-current level that corresponds to 10 % of a gap current surge.

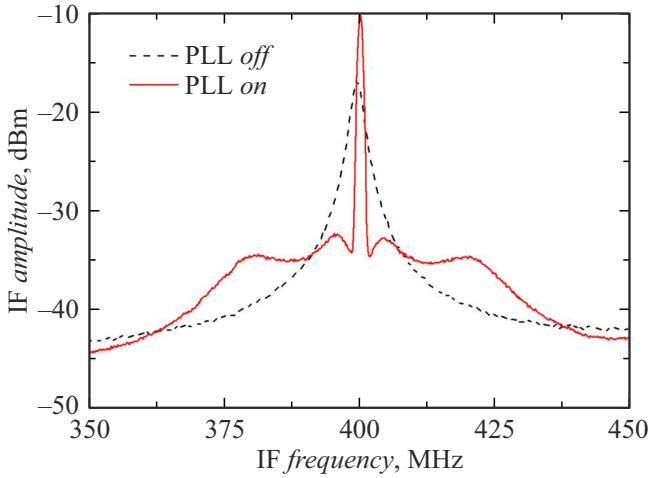

Figure 5. Form of the spectrum at the frequency of 681 GHz. The line width in the free oscillation mode (the black curve) is 2.2 MHz, the signal-to-noise ratio is 27 dB. In the external phase stabilization mode (the red curve), the spectral quality exceeds 80 %.

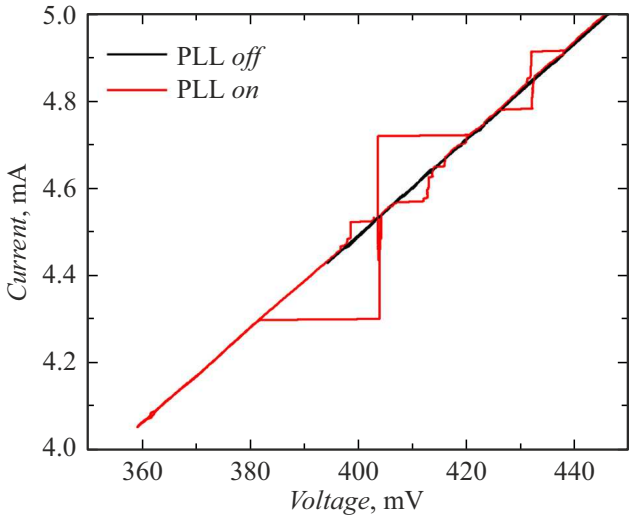

Figure 6. Portion of the current-voltage curve of the array with the operating phase-locked loop system (the red curve) and in the autonomous mode (the black line).

current surge [20]. It should be noted that operation of the mixer included in the heterodyne receiver requires the heterodyne signal power that creates the pump current exceeding 25 % of the gap current surge. It is clear from Fig. 4 that the oscillation power that is sufficient for operation of frequency and phase stabilization can be obtained within the frequency band from 400 to 700 GHz, which is caused by a characteristic of transmission of a match diagram between the array and the SIS mixer. When approximating the current-voltage curve of the SIS mixer with the theoretical expressions from the Tucker-Feldman model [5], the maximum oscillation power was estimated to be 0.12 μW.

3.2. Measurement of the oscillation spectra and implementation of the PLL mode

Fig. 5 shows the array radiation spectrum in the operating point at the frequency of 681 GHz. The signal is output to the spectrum analyzer's display after transforming the signal to the difference frequency f_{IF}. The oscillation line width in the autonomous mode turned out to be about 2 MHz at the signal-to-noise ratio of 27 dB. In the best points, the oscillation line width is below 1 MHz. The data are obtained in the mode of frequency line stabilization with 100 averagings. It should be noted that the signal amplitude at the intermediate frequency also depends on the operating point of the SIS mixer and the synthesizer power. The curves of Fig. 5 are obtained when selecting optimal values of these parameters.

The red solid curve marks the oscillation spectrum with the switched-on mode of phase frequency stabilization. As far as the authors of the present study know, oscillation of the array of the Josephson junctions in the phase-locked loop mode to the stable external synthesizer is implemented for the first time. The spectral quality of the line in this point exceeds 80 %.

Fig. 6 shows the portion of the current-voltage curve of the array with the switched-on phase-locked loop system and without it. The width of the current synchronization area is about 0.4 mA, which is 10 % of the current value in the operating point. These data indicate high efficiency of operation of the phase-locked loop system.

3.3. Internal frequency capture

In order to compare the line width in the experiment with a theoretical value obtained from differential resistance, a series of measurements of the array radiation spectra was carried out within the range from 480 to 500 mV. The voltage interval between the measurements was about 0.25 mV.

A procedure of measurements in each point consists of several actions. First, the operating point is selected in a certain portion of the current-voltage curve of the array by pre-defining the current. Then, the synthesizer frequency is chosen so as to place the difference frequency signal, which is obtained when mixing array radiation with the synthesizer harmonic, around 400 MHz. After that, a number of the harmonic is determined: when mixing the array signal with the i-th harmonic, a change of the synthesizer frequency by 10 MHz will result in shift of the difference frequency by i^*10 MHz. It should be noted that the difference frequency may be shifted both to the right and to the left in relation to the synthesizer. It is due to the fact that the spectrum is measured in the upper $(f_{array} > i f_{synth})$ or lower $(f_{array} < i f_{synth})$ sideband (USB and LSB, respectively). Within the framework of this series of the measurements, the work was carried out only in the lower sideband at the 32-nd harmonic. After that, the synthesizer signal power and voltage at the harmonic SIS mixer were selected so as to provide the largest signal of the intermediate frequency (IF). These parameters were selected only once and then they remained unchanged within the series of the measurements.

During the measurements, in each point after varying the bias current through the array, the synthesizer frequency was again selected so as to set the difference frequency signal at 400 MHz. At the same time, the frequency stabilization system is adjusted so as to keep the line near the difference frequency around 400 MHz. We have tuned the synthesizer frequency in order to unchange the operating point when switching on the frequency stabilization. After that, the signal frequency stabilization system was switched on and averaging across the 100 measurements was activated. Then, the frequency stabilization system was switched off and the array was brought to the new operating point and the procedure was repeated. The frequency stabilization system with an adjustment band of 10 kHz does not change the form of the line and its width.

Each point was taken to measure the current and the voltage at the array as well as the synthesizer frequency and the spectrum itself at the difference frequency. An amplitude of oscillation of the Josephson oscillators near the fundamental frequency has a typical form of the Lorentz curve. That is why when processing each spectrum was approximated by the function (1), from which a position of the oscillation center and the oscillation line width were obtained:

$$A = \frac{A_0}{(f - f_{0,IF})^2 + (\delta f)^2}, \qquad (1)$$

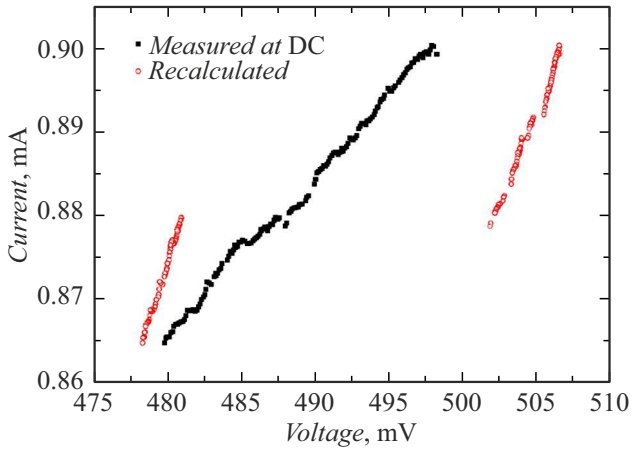

Figure 7. Portion of the current-voltage curve of the array, which is measured at direct current and recalculated from the measurements of the spectrum by the Josephson formula per $N = 350$ junctions. The internal frequency capture is visible.

where $f_{0,IF}$ — the oscillation center position at the difference frequency, δf — the line width.

It should be noted that connection of the PLL system adds a resistance of about 100 Ω in parallel to the array. At the same time, the resistance of the very array made up of the 350 junctions is about 400 Ω. For this reason, the current-voltage curve differs from the measurements that were carried out at direct current in a submersible cryogenic probe. The additional resistance shall be taken into account for correct calculation of the differential resistance of the array.

In order to check applicability of the Josephson formula to description of a relation between the oscillation frequency and the array voltage, the frequency determined by the spectrum analyzer was converted into the voltage by the formula

$$V_s = \frac{h}{2e}(i f_{synth} - f_{0,IF}). \qquad (2)$$

The sign „–“ in front of the intermediate frequency $f_{0,IF}$ is due to operation in the lower sideband (LSB).

The portion of the array's current-voltage curve that is measured at direct current (the black dots) as well as the current-voltage curve recalculated from the spectral measurements (the red dots) are shown in Fig. 7. As can be seen, the current-voltage curves measured by the two methods differ considerably.

During the measurements, both the harmonic number and the operating sideband remained unchanged. Most likely, the discrepancy is caused by internal array oscillation frequency capture when the oscillation frequency is quite close to the frequency of the resonance mode in the coplanar line [16]. The distance between the resonance

modes can be calculated by the formula

$$\Delta f = \frac{v}{2L} \sim \frac{c}{2L}\sqrt{\frac{2}{\varepsilon + 1}}, \tag{3}$$

where v — the speed of propagation of the wave in the coplanar line, c — the speed of light in vacuum, L — the length of a portion, in which the standing waves are formed, $\varepsilon = 11.7$ — permittivity of the silicon substrate, on which the sample is manufactured.

As can be seen in Fig. 7, the distance between the portions of the current-voltage curve, which are recalculated by the Josephson formula, is about 19 mV, which corresponds to the frequency of 27 GHz. With the length of the coplanar line $L = 2$ mm, it was calculated by the formula (3) to give the value 30 GHz, which coincides with the measured value taking into account dispersion of permittivity in the coplanar line [21]

It should be noted that the array made up of 350 junctions consists of two sections — 200 and 150 junctions of the length of 2 and 1.5 mm, respectively, which are separated by rotation by 180° (Fig. 1, *b*). The portion of the circuit with the harmonic mixer is connected to the section with 200 junctions and it is the length of this section, by which the resonance frequencies are determined.

Besides, the recalculated current-voltage curve has exhibited four additional portions, between which a frequency surge is detected and oscillation can not be measured. At the same time, the oscillation line width in these portions increases from the middle to the edges. A cause of origin of this „fine structure“ is subject to further investigation.

3.4. Comparison of the oscillation line width with the theoretical models

Fig. 8 compares the experimentally-obtained values of the oscillation line width with the calculations. The black dots with error bars correspond to the experimental values, while the red circles correspond to the theoretical values.

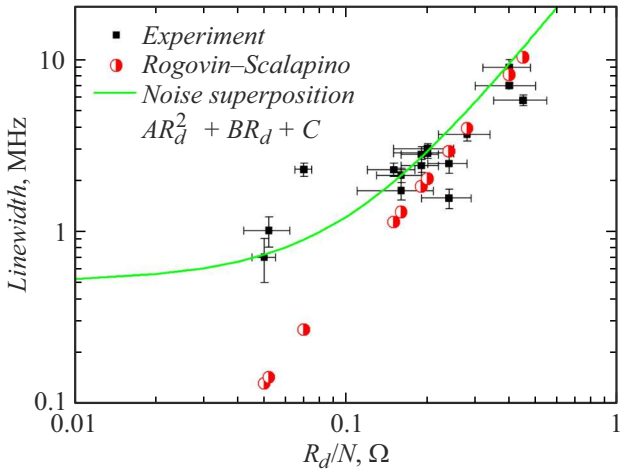

Figure 8. Dependence of the oscillation line width on the differential resistance in the operating points at the various array voltages. The parameters of the green curve: $A = 50$, $B = 2$, $C = 0.5$.

As follows from the fluctuation-dissipation theorem, the dependence of the oscillation line width is quadratic in R_d. In case of one junction, an exact value of the coefficient of proportionality can be determined by the formula from the Rogovin-Scalapino model [22]:

$$\delta f = \left(\frac{4\pi e}{h}\right)^2 R_d^2 S_I(0), \tag{4}$$

where $S_I(0)$ is the noise spectral density at the zero frequency. This value includes several components: noise directly at the junctions in the array $S_{I,2}(0)$, low-frequency noise affecting the array $S_{I,1}(0)$ and thermal noise, in particular, on the shunts $S_{I,0}(0)$. The full noise spectral density in the formula (4) will be obtained by summing all the components.

$$S_{I,2}(0) = \frac{e}{2\pi}\left(I_{qp}\coth\left(\frac{eV_0}{2k_BT}\right) + 2I_p\coth\left(\frac{eV_0}{k_BT}\right)\right),$$

$$S_{I,0}(0) = \frac{e}{2\pi}I_{qp}\left(\frac{R_N}{R_d}\right)^2, \tag{5}$$

where I_{qp} and I_p — the quasi-particle current and the Copper pair current, respectively; V_0 — the voltage at the junction in the operating point, T — the temperature in the experiment, R_N — the active resistance of the shunts. At the voltages below the gap voltage, the quasi-particle current in the tunnel junction is quite small: a ratio of the differential resistance to the normal resistance exceeds 20. Therefore, within the estimates done we have assumed that I_{qp} is much less than I_p, which is equal to the critical current in order of magnitude.

As said above, in case of the array made up of N junctions it is expected that the value of δf will be in N times less. The red dots in Fig. 8 are obtained by the substitution $S_I(0) = S_{I,2}(0)$. The experimental and theoretical values coincide within experiment errors when the values of R_d exceed 0.1 Ω.

With the smaller values of the differential resistance, the thermal and low-frequency noises in the system result in broadening of the line. Qualitatively, it is possible to take into account thermal noises by introducing an additional summand that does not depend on R_d. But presence of low-frequency fluctuations, which can not be suppressed by the frequency stabilization system, results in emergence of a summand that is linear by R_d. The function of the form $y(R_d) = A \cdot R_d^2 + B \cdot R_d + C$ is shown in Fig. 8 by the green line [23]. Here, A, B and C are certain dimensional parameters that are related to respective spectral densities of the fluctuations. Detailed theoretical description will be also be presented in the future.

Conclusion

The study has investigated the spectral properties of the terahertz-range superconducting oscillator based on

the array of the Josephson junctions embedded into the central electrode of the coplanar line. The procedure of measurement of the array oscillation spectra has been tested when mixing the array signal with radiation arriving from the synthesizer on the harmonic mixer. In the best points, the oscillation line width is below 1 MHz. For the values of the differential resistance per one junction, which exceed 0.1 Ω, the experimental values of the line oscillation width coincide within the error with those theoretically calculated by the Rogovin-Scalapino formula that is normalized to the number of the junctions in the array. The difference with small R_d can be explained by taking into account additional thermal and low-frequency noises in the system.

We were the first ones to demonstrate the phase-locked loop of the oscillator based on the array of the Josephson junctions to the stable external source. The signal spectral quality in the phase-locked loop mode exceeds 80 %. At the same time, the current synchronization area exceeds 10 % of the current value in the operating point.

The spectrum measurements were taken to detect frequency oscillation capture that is due to interaction of the junctions with radiation in the coplanar line. This effect is manifested in that with continuous variation of the array voltage the oscillation frequency varies unproportionally to the voltage, but when exceeding a certain value it experiences switching from one mode of the coplanar line into another. Besides, several areas were observed within one series without flipping between the modes, between which no radiation was detected, but within each area the line width increased from the middle to the edges. This issue will be studied in the future.

The heterodyne oscillator requires that the frequency can be continuously retuned. Consequently, the samples are designed with the concerted load on a non-emitting end. Thus, another step has been made for creation of the superconducting integrated heterodyne oscillator based on the array of the Josephson junctions.

Funding

This study was supported by the Ministry of Science and Higher Education of the Russian Federation (Agreement № 075-15-2024-538).

Acknowledgments

All the samples were made using a unique scientific plant „Criointegral“ (UNU№352529) of the Kotelnikov Institute of Radioengineering and Electronics of the Russian Academy of Sciences.

Conflict of interest

The authors declare that they have no conflict of interest.

References

[1] *ALMA Space observatory Website.* Available online: https://www.almaobservatory.org/
[2] *Apex Space Telescope Website.* Available online: http://www.apex-telescope.org/
[3] *Hershel Space Telescope Website.* Available online: https://www.herschel.caltech.edu/
[4] *„Millimetron“ space observatory website.* Available online: https://millimetron.ru/
[5] J.R. Tucker, M.J. Feldman. Rev. Modern Phys., **57** (4), 1055 (1985). DOI: 10.1103/RevModPhys.57.1055
[6] A.R. Kerr, M.J. Feldman, S.-K. Pan, *Proceedings of the Eighth International Symposium on Space Terahertz Technology* (Cambridge, MA, USA, 1997)
[7] M. Tinkham *Introduction to Superconductivity*, 2nd edition (McGraw-Hill, 1996), p. 77.
[8] J.V. Siles, K.B. Cooper, C. Lee, R.H. Lin, G. Chattopadhyay, I. Mehdi. IEEE Trans. Terahertz Sci. Technol., **8** (6), 596 (2018).
[9] V.P. Koshelets, S.V. Shitov, A.B. Ermakov, L.V. Filippenko, O.V. Koryukin, A.V. Khudchenko, M.Yu. Torgashin, P.A. Yagoubov, R.W.M. Hoogeveen, O.M. Pylypenko. IEEE Trans. Appl. Supercond., **15** (2), 960 (2005). DOI: 10.1109/TASC.2005.850138
[10] N.V. Kinev, K.I. Rudakov, L.V. Filippenko, A.M. Baryshev, V.P. Koshelets. Sensors, **20** (24), 7267 (2020). DOI: 10.3390/s20247267
[11] K.A. Baksheeva, R.V. Ozhegov, G.N. Goltsman, N.V. Kinev, V.P. Koshelets, A. Kochnev, N. Betzalel, A. Puzenko, P.B. Ishai, Yu. Feldman. IEEE Trans. Terahertz Sci. Technol., **11** (4), 381 (2021). DOI: 10.1109/TTHZ.2021.3066099
[12] V.P. Koshelets, S.V. Shitov, A.V. Shchukin, L.V. Filippenko, J. Mygind, A.V. Ustinov. Phys. Rev. B, **56** (9), 5572 (1997). DOI: 10.1103/PhysRevB.56.5572
[13] D.D. Coon, M.D. Fiske. Phys. Rev., **138** (3A), A744 (1965). DOI: 10.1103/PhysRev.138.A744
[14] A.K. Jain, K.K. Likharev, J.E. Lukens, J.E. Sauvageau. Phys. Reports, **109** (6), 309 (1984). DOI: 10.1016/0370-1573(84)90002-4
[15] M. Darula, T. Doderer, S. Beuven. Supercond. Sci. Technol., **12** (1), R1 (1999). DOI: 10.1088/0953-2048/12/1/001
[16] M.A. Galin, I.A. Shereshevsky, N.K. Vdovicheva, V.V. Kurin. Supercond. Sci. Technol., **34** (7), 075005 (2021). DOI: 10.1088/1361-6668/abfd0b
[17] A. Kawakami, Y. Uzawa, Z. Wang. IEEE Transactions Appl. Supercond., **9** (2), 4554 (1999). DOI: 10.1109/77.784039
[18] F.V. Khan, L.V. Filippenko, A.B. Ermakov, M.E. Paramonov, M.Yu. Fominskii, N.V. Kinev, V.P. Koshelets, S.A. Nikitov. UFN, **195** (6), 621(2025) (in Russian). DOI: 10.3367/UFNr.2024.12.039864
[19] L.V. Filippenko, S.V. Shitov, P.N. Dmitriev, A.B. Ermakov, V.P. Koshelets, J.R. Gao. IEEE Trans. Appl. Supercond., **11** (1), 816 (2001). DOI: 10.1109/77.919469
[20] V.P. Koshelets, S.V. Shitov, P.N. Dmitriev, A.B. Ermakov, L.V. Filippenko, V.V. Khodos, V.L. Vaks, A.M Baryshev, P.R. Wesselius, J. Mygind. Physica C: Superconductivity, **367** (1), 249 (2002). DOI: 10.1016/S0921-4534(01)01046-2

[21] D. Mirshekar-Syahkal, J.B. Davies. IEEE Transactions on Microwave Theory and Techniques, **27** (7), 694 (2003). DOI: 10.1109/TMTT.1979.1129703
[22] D. Rogovin, D.J. Scalapino. Annals Physics, **86** (1), 1 (1974). DOI: 10.1016/0003-4916(74)90430-8
[23] K.K. Likharev. *Dynamics of Josephson junctions and circuits.* (Gordon and Breach science publishers, NY., 1986), p. 98.

Translated by M.Shevelev